ACS APPLIED ELECTRONIC MATERIALS

pubs.acs.org/acsaelm Article

Layer-by-Layer Assembly Monitored by PEDOT-Polyamine-Based Organic Electrochemical Transistors

Gonzalo Eduardo Fenoy,* Juliana Scotto, Juan A. Allegretto, Esteban Piccinini, Agustín Lorenzo Cantillo, Wolfgang Knoll, Omar Azzaroni, and Waldemar Alejandro Marmisollé*

Cite This: https://doi.org/10.1021/acsaelm.2c01124 Read Online

ACCESS | Metrics & More | Article Recommendations | Supporting Information

ABSTRACT: In this work, we present the fabrication of PEDOT−PAH-based organic electrochemical transistors (OECTs), that are employed to monitor the deposition of polyelectrolyte multilayers on their surface. We first explore different synthesis conditions in order to optimize the electrical characteristics of the devices, such as threshold voltage and voltage of maximum transconductance. Next, the transistors showing the desired features are chosen to investigate the process of the layer-by-layer (LbL) assembly through (i) the analysis of the transfer characteristics curves and (ii) the changes in the registered drain−source current. It is demonstrated that the OECTs are able to monitor the assembly of the different polyelectrolyte layers in real time in both modes of operation, yielding information about conductivity and surface potential changes in the channel. Next, the transient characteristics of the devices are studied upon the assembly of the different layers, providing information about the changes in the ionic transport through the whole film during the ON and OFF switching. Finally, the kinetic response of the OECTs toward the monitoring of charged macromolecules is fitted to a two-step adsorption model and compared against graphene field-effect transistors and surface plasmon resonance. The monitoring of the LbL assembly by the changes in the PEDOT−PAH OECT response illustrates the use of these transistors for sensing interactions with charged species in solution and supports the development of sensing platforms by integration of specific recognition elements on the conducting polymer channel.

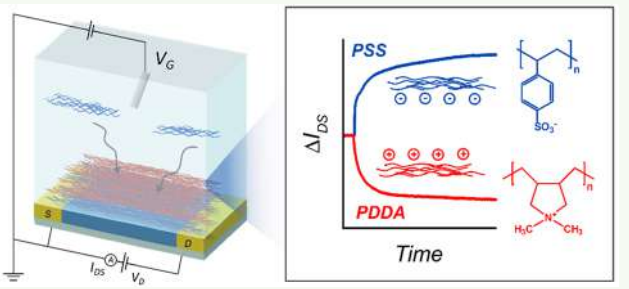

KEYWORDS: *organic electrochemical transistors, layer-by-layer, polyelectrolyte multilayers, PEDOT, polyamines*

INTRODUCTION

The development of organic bioelectronic devices involves the design of transducing platforms operating at the interface between biological systems and data acquisition and processing apparatuses.[1] The fabrication of said devices is achieved through the effective connection between organic semiconductors and biological entities of all sizes and shapes, from small molecules, proteins, and membranes to cells, tissues, organs, and living organisms.[2,3] During the last decades, the better understanding of mixed ionic/electronic transport properties, the advancement of fabrication techniques, and the innovation in the design and synthesis of novel materials have driven remarkable progress in this field.[4,5] Therefore, several devices such as biosensors,[6] soft actuators,[7] recording and stimulation probes,[8] and organic electrochemical transistors (OECTs)[9] have been developed, allowing for the detection of biomarkers, the recording of electrophysiological signals, and the stimulation of cells, among other interesting applications.[10,11]

In OECTs, particularly, source and drain electrodes are connected through an organic semiconducting channel, whose conductivity is modulated by the application of a gate voltage (V_G) through an electrolyte.[12,13] OECTs can, therefore, operate under two regimes: at a certain range of applied V_G, they behave as electronic conductors (ON state), whereas in other V_G range their conductivity is comparatively low (OFF state). The rate of change of the conductivity with the gate voltage is called transconductance (g_m). The occurrence of ion injection from the electrolyte to maintain charge balance in the organic film makes these devices work as organic mixed ionic−electronic conductors (OMIECs) and provides them with record-high transconductance, whereas it also limits their response time.[14,15]

During the last years, poly(3,4-ethylenedioxythiophene):poly(styrenesulfonate) (PEDOT:PSS) has been widely employed as a conducting channel for the fabrication of OECTs.[16] However, its intrinsic doping causes the operation

Received: August 25, 2022
Accepted: November 7, 2022

of the devices in depletion mode, demanding high operating currents and elevated gate voltages to maintain the channel in the OFF state.[17] Moreover, the application of these relatively high voltages when operating through an electrolyte can generate parasitic reactions with water and oxygen, causing the deterioration of the transistors.[4,18] In addition, concerning the integration with biological systems, PEDOT:PSS exhibits some disadvantages due to the acidity/toxicity of PSS and the relatively low biocompatibility of PEDOT.[19,20] Since PSS is usually in excess in the conducting polymer−polyelectrolyte complex, its overall negative charge limits its interfacing with most of the cells, nucleic acids, and proteins, since they are also negatively charged at physiological conditions.[21,22]

Regarding this aspect, the addition of polyamines to the channel material of PEDOT-based OECTs has been reported as an efficient method to overcome some of the above-mentioned limitations.[4,19] For instance, it has been demonstrated that the operation voltage range of OECTs can be simply modulated by dedoping with polyethylenimine (PEI) and also with vapors of commercially available aliphatic amines.[18,23] Moreover, Cea et al. have recently developed enhancement-mode ion-gated OECTs by making use of a PEDOT:PSS/PEI blend as channel material.[24] In addition, we have recently shown that the threshold voltage (V_{th}) of OECTs made of PEDOT and tosylate dopant (PEDOT:TOS) can be easily modulated by the addition of poly(allylamine hydrochloride) (PAH) to the conducting channel, while also allowing for the anchoring of enzymes on the surface through the incorporation of amine moieties.[9]

Regarding strategies for surface functionalization, the layer-by-layer assembly (LbL) technique appears as a straightforward approach for the deposition of macromolecules with multiple charges to form multilayers in a controlled manner.[25] This technique was first described by Decher et al.,[26] and, although it was originally established for the construction of polyelectrolyte multilayers, nowadays it has been expanded to a great variety of materials and surfaces.[27−29] When making use of the LbL technique, the alternate deposition of building blocks avoids undesirable consequences such as aggregation and allows intimate contact between the different film constituting elements, features that are crucial for efficient transport properties.[27,30] Therefore, LbL-interfacial nanoarchitectures exhibiting the integration of diverse materials into structurally stable and functional interfacial systems have received increased attention from the scientific community, showing great performance in applications related to energy storage and conversion, catalysis, and biosensing technologies.[31,32]

While several interactions have been used for the construction of multilayer thin-film architectures, such as hydrogen bonding and/or van der Waals "soft" interactions,[32−34] the use of electrostatic forces to drive the assembly of polyelectrolyte multilayer continues to be the most employed strategy to fabricate films through the LbL technique.[29,35] In this context, it has been previously shown that the alternated assembly of polyelectrolytes results in a straightforward and useful proof-of-concept approach for the development of biosensing FET-based devices, such as those based on graphene field effect transistors.[36−38]

In this context, the monitoring of the adsorption of charged molecules has been demonstrated to be of major importance for the development of accurate biosensing devices.[36,39] Particularly, in field-effect transistor-based biosensors, the current transported by the conductive channel is sensitive to the presence (and variation) of electric fields in the vicinity of its surface, which constitutes the main signal transduction mechanism of these devices.[6,36] Then, through the adequate design and use of surface coatings on the conductive channel, it is possible to transduce a molecular phenomenon of interest into changes of the electronic response of these devices. In this regard, OECTs have been employed for the detection of a wide range of analytes from single ions to proteins,[40,41] protein aggregates,[42] and even virus particles.[43] As far as we know, there has been only one previous report for the deposition of polyelectrolyte LbL assemblies on OECTs.[44] In that work, the authors employed PEDOT:PSS-based OECTs and studied the LbL assembly of polyelectrolytes in diluted buffer (0.1× PBS or 0.01× PBS). Nevertheless, the kinetic response during the adsorption of the polyelectrolytes was not studied.

In this work, we fabricate polyamine-PEDOT-based OECTs and study the assembly process of polyelectrolyte multilayer thin films on these devices. First, we adjust the thickness of the conducting channel with the aim of optimizing relevant OECT features such as threshold voltage, transconductance, and voltage of maximum transconductance. Next, the incorporation of the polyamine in the conducting channel allows the direct adsorption of polyelectrolyte layers onto the channel and the monitoring in real time of the multilayer assembly process by means of the changes in the recorded drain−source current. Furthermore, the effect of the assembled multilayer film on the transient response of the devices is studied, elucidating the different ionic and electronic transport processes that participate in the response of the devices. Lastly, a two-step model is employed to fit the kinetic response of the OECTs toward the monitoring of charged macromolecules and benchmark them against graphene field-effect transistors and surface plasmon resonance determinations. To the best of our knowledge, this is the first time that the real-time monitoring of the assembly of polyelectrolyte multilayers by organic electrochemical transistors is reported, illustrating their capability for the real-time monitoring of molecular events, and having big implications in the development of OECT-based biosensing devices.

MATERIALS AND METHODS

Reagents and Materials. Ethanol, KOH pellets, HCl, 3,4-ethylenedioxythiophene (EDOT) (97%), poly(allylamine hydrochloride) (M_w ∼58 kDa), poly(sodium 4-styrenesulfonate) (M_w ∼70.000) (PSS), and poly(diallyldimethylammonium chloride) solution (average M_w ∼100.000−200.000), 20% in H_2O (PDDA), were obtained from Sigma-Aldrich. Pyridine (99%) was purchased from Biopack, and iron(III) *p*-toluenesulfonate (38−42% in *n*-butanol) was obtained from Heraeus, while *n*-butanol (99.4%), acetone, and KCl were purchased from Anedra. All solutions were prepared with Milli-Q water. Interdigitated electrodes (IDEs) were obtained from Micrux (ED-IDE1-Au, 10/10 μm electrode/gap).

OECT Fabrication and Synthesis Optimization. The OECTs were fabricated based on a previously reported protocol,[9] although some variations were introduced in order to modulate the threshold voltage of the devices (and, therefore, the voltage of maximum transconductance). The protocol is described as follows: First, commercial interdigitated gold electrodes (Micrux, ED-IDE1-Au, 10/10 μm electrode/gap, each IDE consisting of 90 pairs of interdigitated gold electrodes) (IDEs) were cleaned with acetone and ethanol and dried. Next, *in situ* chemical polymerization of PEDOT−PAH on the interdigitated electrode area of the substrates was performed. To this end, an oxidant solution containing 715 μL of 40% Fe(III) tosylate butanol solution, 220 μL of butanol, and 16.5 μL

https://doi.org/10.1021/acsaelm.2c01124
ACS Appl. Electron. Mater. XXXX, XXX, XXX−XXX

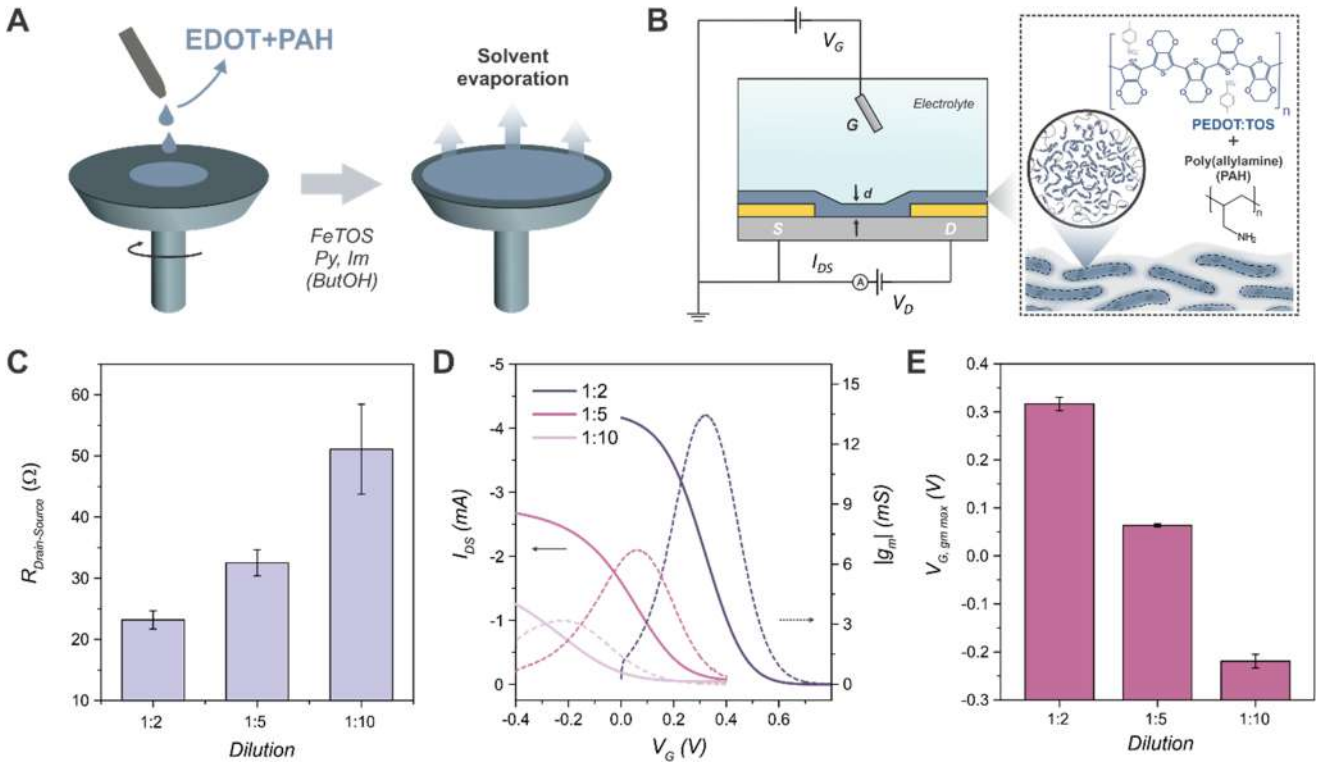

Figure 1. Scheme for the spin-coating process employed to fabricate the OECTs (A). Measurement setup employed for the characterization of the OECTs and illustration of the channel structure (B). Resistance between source and drain electrodes measured in dry conditions immediately after the fabrication of the transistors (C). Transfer characteristics (full lines, left axis) and transconductance (dotted lines, right axis) of the obtained devices from different dilutions (V_D = −100 mV, 0.1 M KCl) (D). Voltage of maximum transconductance for the transistors obtained employing the different conditions (average of three devices, bars correspond to the SD) (E).

of pyridine was prepared. Later, this solution was mixed with 200 μL of 15 mg/mL PAH (57 kDa) and homogenized. Next, 12.5 μL of the EDOT monomer was added, and the solution was homogenized in a vortex and filtered (0.2 μm). After the filtration step, different dilutions with butanol were performed, either 1:2 (i.e., as used in the previously reported protocol[9]), 1:5, or 1:10. Next, the diluted solution was spin coated onto the array area of the substrates at 1000 rpm for 1 min applying an acceleration of 500 rpm min^{-1}. Finally, the substrates were heated at 70 °C for 15 min for producing the polymerization of EDOT to PEDOT, rinsed with Milli-Q water, and dried with N_2.

Layer-by-Layer Assembly Process. The layer-by-layer assembly process was started by making use of the amino moieties of the PEDOT−PAH OECTs as anchoring groups. For the real-time measurements, the necessary volume of 2 mg/mL of PSS and PDDA stock solutions in 0.1 M KCl was added to the measurement cell with 0.1 M KCl to reach a final polyelectrolyte concentration of 0.1 mg/mL, and the transistors were incubated for 20 min (or 40 min in the case of the first PSS layer). Next, for the study of the transfer and the transient characteristics, the modified OECTs were rinsed with Milli-Q water, dried with N_2, and employed for the measurements.

QCM Measurements. Quartz crystal microbalance (QCM) measurements were performed with a QCM200 setup (Stanford Research Systems) using gold-coated quartz sensors (QCM25 5 MHz, sensitivity factor: 56.6 Hz cm^2 μg^{-1}). First, a PEDOT−PAH film was deposited on previously cleaned QCM substrates (three-step washing with acetone, ethanol, and Milli-Q water under sonication) by making use of the same protocol employed for the OECT fabrication (1:5 dilution). PSS and PDDA polyelectrolyte layers were assembled by soaking the quartz sensor for 15 min in 0.1 mg/mL polyelectrolyte solutions in 0.1 M KCl. After each assembled layer, the QCM sensor was rinsed and dried under N_2. Measurements were conducted on dry conditions, thus avoiding viscoelastic contributions from the media.

Electrical Measurements. The resistance of the channel of the as-synthesized OECTs was measured with an Agilent Technologies U1241A multimeter after the transistors were prepared. The output, transfer, and transient characteristics of the transistors were obtained employing a TEQ bipotentiostat. The electrochemical cell used consisted of a batch add-on cell obtained from Micrux Technologies, and a Ag/AgCl (3 M KCl) electrode was used as the gate. All the measurements were performed in 0.1 M KCl, pH 7 electrolyte.

RESULTS AND DISCUSSION

OECT Fabrication and Optimization. The first step of the work involved the fabrication of PEDOT-polyamine-based transistors employing different synthesis conditions in order to optimize their performance by adjusting a previously reported protocol.[9] It has been shown that the threshold voltage of OECTs can be easily tuned by modulating channel parameters such as width/length (W/L) ratio and thickness.[45] In this regard, lowering the threshold voltage reduces the power consumption and may simplify the readout circuit design by using only one power supply. Moreover, it also improves the stability of the bioentities, such as proteins, lipid bilayers, or cells, which could degrade at high applied voltages.[46] More importantly, the operation of the transistors at gate voltage (V_G) ≈ 0 V prevents the alteration of the deposition process of the layer-by-layer assembly, since it is known that the process could be distorted upon the application of high electrical fields (the so-called electrophoretic LbL deposition).[47]

PEDOT−PAH OECTs were fabricated *in situ* by chemical polymerization of the channel material on commercial IDEs by spin coating (Figure 1(A) and (B)). In order to optimize the threshold voltage of the transistors (and therefore the

https://doi.org/10.1021/acsaelm.2c01124
ACS Appl. Electron. Mater. XXXX, XXX, XXX−XXX

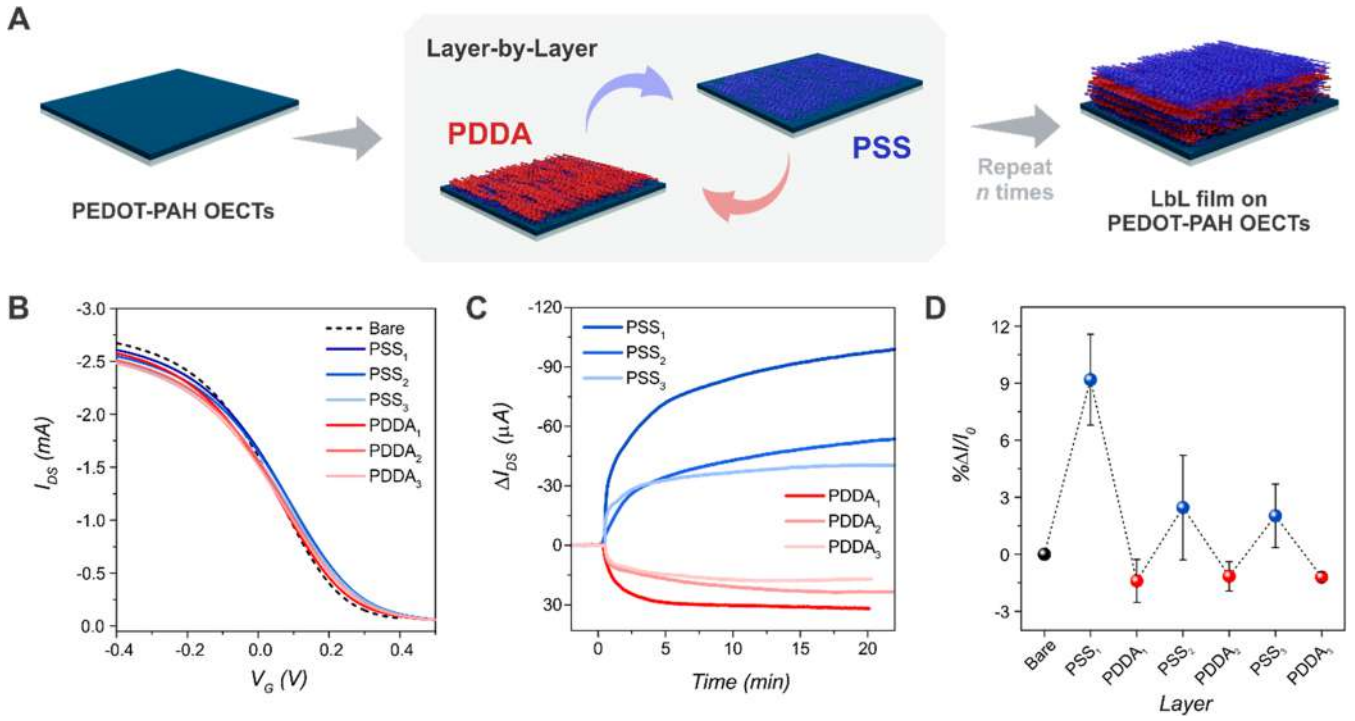

Figure 2. Scheme of the layer-by-layer assembly process on OECTs (A). Transfer characteristics for an OECT upon the assembly of different polyelectrolyte layers (V_D = −0.1 V, KCl 0.1 M) (B). Real-time monitoring of the layer-by-layer assembly process by the OECTs measured as the change in I_{DS} (V_G = 0 V, V_D = −0.1 V, KCl 0.1 M) (C). Results for relative change in I_{DS} upon the injection of polyelectrolyte solutions for two different OECTs (bars correspond to the SD) (D). For both polyelectrolytes, the concentration during the assembly is 0.1 mg/mL and the supporting electrolyte is 0.1 M KCl.

maximum transconductance voltage, $V_{G,\,gm\,max}$[45]), the concentration of the synthesis solution was varied by performing different dilutions in butanol. Figure 1(C) shows the resistance measured in air at room temperature between both source and drain electrodes immediately after the fabrication of the OECTs, while the transfer characteristics of the obtained devices can be observed in Figure 1(D).

All the obtained OECTs show the typical features of depletion mode transistors (i.e., in the absence of a gate voltage, the devices display the ON state). However, significant differences in terms of resistance and transfer characteristics are observed depending on the dilution employed during synthesis. First, the resistance of the as-prepared transistors increases with the dilution of the synthesis solution. On the contrary, the values of the drain−source current (I_{DS}) of the ON state decrease as the synthesis solution is diluted. These results support the idea that OECTs with thinner conducting channels are obtained while performing further dilutions of the synthesis solution. On the other hand, the reproducibility of the fabrication procedure decreases as the synthesis solution is diluted; the transistors obtained with the 1:5 dilution preserve a relatively low RSD of the measured resistance in the dry state (6.5%), whereas this value increases for the 1:10 dilution (14.4%). Moreover, the OECTs fabricated by making use of the 1:10 dilution showed degradation over the repeated cycling of the transfer characteristics, as shown in Figure S1, while this effect was not observed for the OECTs synthesized employing the 1:5 dilution.

Furthermore, Figure 1(D) also shows the transconductance values for the transistors obtained for each synthesis condition. It can be observed that the maximum transconductance of the devices diminishes as the dilution increases (in line with the diminution of ON I_{DS}). This result is indicative of the reduction of the thickness of the polyelectrolyte-conducting polymer channel film. Similarly, the threshold voltage decreases in a similar fashion to that observed for the $V_{G,\,gm\,max}$ (Figure S2). The tuning of the threshold voltage (and therefore the $V_{G,\,gm\,max}$) by controlling the thickness of the transistors (while keeping the channel length and width constant) has been reported as an efficient way to obtain zero-gate bias devices.[45] Figure 1(E) shows the values obtained for the $V_{G,\,gm\,max}$ for three different synthesis conditions. It can be observed that the transistors fabricated by making use of the 1:5 dilution show a $V_{G,\,gm\,max}$ value close to 0 V. Together with the relatively good reproducibility and stability, these outcomes motivate the selection of the 1:5 synthesis dilution fabricated transistors to evaluate the OECTs' performance for the monitoring of the charged macromolecules.

Layer-by-Layer Assembly Monitoring by OECTs. The devices fabricated with the 1:5 dilution were subsequently employed to monitor the assembly of polyelectrolyte multilayers constructed by the LbL method. The presence of the polyamine in the conducting channel avoided the requirement of an extra step to functionalize the channel, and the assembly process therefore started with a layer of the polyanion poly(sodium 4-styrenesulfonate) (PSS). Subsequently, the polycation poly(diallyldimethylammonium chloride) (PDDA) was assembled, and the bilayer assembly process was repeated three times, yielding a $(PSS/PDDA)_3$ assembly (Figure 2(A) and Supporting Information). The transfer characteristics of the devices were evaluated after each layer deposition, whereas the assembly process was also monitored in real time by registering the I_{DS} current after the addition of the polyelectrolyte solution. Figure 2(B) shows the transfer

https://doi.org/10.1021/acsaelm.2c01124
ACS Appl. Electron. Mater. XXXX, XXX, XXX−XXX

characteristics of a PEDOT−PAH OECT upon the successive polyelectrolyte layer depositions up to three assembled bilayers, while Figure S3 shows the shift of the gate voltage with respect to the bare OECT. For the transfer characteristics, the values for the gate voltage shifting were computed as the shift relative to the current value for V_G = 0 V of the bare PEDOT−PAH transistors (as described in the Supporting Information). Regarding the real-time monitoring of the assembly process, the values were computed as the relative change (ΔI_{DS}) with respect to the initial current value (I_0) in order to consider differences that could arise in these values for the different devices.

Figure 2(B) shows that the transfer curve shifts to more positive gate potentials upon the deposition of the PSS layers, while a shift to more negative gate potentials is observed upon the deposition of the PDDA layers. Moreover, both effects occur for all the assembled layers studied here (three bilayers). These results can be explained as follows: the fabricated OECTs are comprised of a channel material that contains a blend of both PEDOT:TOS and PAH polymers. In this regard, it has been widely demonstrated that polyamines such as PEI and PAH, as well as vapors of commercially available aliphatic amines, can dedope PEDOT-based OECTs, yielding noticeable changes in the threshold voltage of the devices.[23,48] Next, when the first layer of the PSS polyanion is deposited, it changes the electrostatic surface potential due to the creation of negative surface charges. As a consequence, the effective gate voltage on the electroactive film is also shifted. As recently shown,[9] the V_{th} of the PEDOT−PAH films does correlate with the apparent redox potential of the film. The shifting in the effective gate voltage on the electroactive film means a change of the apparent redox potential when the Ag/AgCl gate electrode is considered as reference. Then, higher gate voltages are needed to produce the same reduction degree of the PEDOT−PAH film, causing a shift of the transfer curve to higher V_G values.

In this regard, the effect of the zeta-potential of the film on the apparent redox potential of an electroactive species inside the film has been also reported for the LbL assembly of redox polymers.[49,50] In those cases, an alternating shift is observed depending on the charge of the outermost layer. The surface charge reversion has been extensively reported for the LbL formation on flat surfaces or colloidal particles, and it yields an alternation of the zeta-potential values between positive and negative values.[51,52] In the present case, when a PDDA layer is subsequently assembled on the surface, the polycation overcompensates the negative charges of PSS. The positive surface charge now shifts the effective gate voltage in the opposite direction. As a consequence, lower gate voltages are required to produce a certain reduction degree and the transfer curve moves toward lower V_G values. A similar trend has been reported for the LbL deposition of polyelectrolytes on gFETs.[37,53] Next, the sequential assembly of the multilayer film is observed as an alternating positive and negative shift in the gate voltage with respect to the gate voltage value of bare OECTs. Moreover, similar outcomes are also observed when performing measurements at a fixed gate potential (V_G = 0 V), as shown in Figure 2(C) and (D). In this configuration, an increase of the current is observed upon the deposition of a PSS layer, as it is expected considering the shift of the transfer curve to more positive gate voltages (while the opposite is observed for the deposition of PDDA layers).

In addition, it can be seen from Figure 2(C) and (D) that the first layer of PSS generates a larger change in I_{DS} compared to those observed for the subsequent layers. Since the conducting channel of the transistors is comprised of more PAH than PEDOT (for the synthesis conditions employed the PAH/PEDOT ratio has been determined as 1.34[9]), the first layer of PSS compensates the cationic charges of the polyamine in the channel composite material and allows for more TOS^- anions to stabilize the hole-conducting state of PEDOT, which results in a shift of the transfer curve to more positive gate voltages.[44,54] Thus, this doping effect would be additive to the zeta-potential electrostatic effect. On the other hand, when the subsequent PDDA layer is deposited, the positive charges only compensate the negative charges in excess and do not affect the PEDOT doping itself. In line with those findings, it can be noticed that the change in the registered current for the assembly of the first layer of PSS also takes more time to reach the so-called plateau (while the curve with the complete time scale is shown in Figure S4). For the deposition of the rest of the layers, the layer assembly process reaches the plateau in a time frame of up to 10 min, in good agreement with previously reported results for the real-time study of the LbL assembly process by making use of SPR and QCM techniques.[32,36] Therefore, we hypothesize that the change in the conductivity of the channel could be restricted to the deposition of the first layer (PSS), which compensates the excess of PAH in the polymer blend (molecular doping effect). In this regard, during the first soaking in the PSS solution, the negatively charged polyelectrolyte would interpenetrate into the PEDOT−PAH channels as well as adsorb on the channels' surface, causing a bulk doping effect additional to the reversion of the surface zeta potential.

This hypothesis is supported by the two facts previously mentioned, i.e., the longer time necessary to reach the plateau for this layer compared to the rest of the assembly as well as the larger change in I_{DS}. This explanation is also consistent with a higher amount of PSS deposited in the first modification step as compared with the following polyelectrolyte layers as revealed by QCM (see the Supporting Information). Subsequently, after the adsorption of the first PSS layer, the shift in the gate voltage caused by the deposition of the subsequent charged polymer layers could be ascribed to a shift in the surface potential of the transistor's channel, which depends on the nature of the charged species. Next, the adsorption of both charged polyelectrolytes is observed as the LbL assembly continues, yielding alternated increases and diminutions for the registered I_{DS} at V_G = 0 V (Figure 2(C) and (D)). In this regard, the adsorption of charged polymer layers has been reported to shift the surface potential of different FET-based devices, such as graphene field-effect transistors and Si-based ISFETS.[37,54]

In addition, the continuous monitoring of the I_{DS} changes upon the different deposition cycles was performed by injecting the polyelectrolytes under flow conditions, until a six-bilayer assembly was obtained (Figures S5 and S6). The results of this experiment were very similar to those obtained in the static condition, showing alternate increases and decreases in I_{DS} upon PSS and PDDA adsorption, respectively.

It is worth noting here that the low threshold voltage of these transistors (and therefore their apparent redox potential) allows to carry out the polyelectrolyte adsorption process without significantly modifying the electric field on the surface of the channel. Thus, the polyelectrolyte assembly can be

https://doi.org/10.1021/acsaelm.2c01124
ACS Appl. Electron. Mater. XXXX, XXX, XXX−XXX

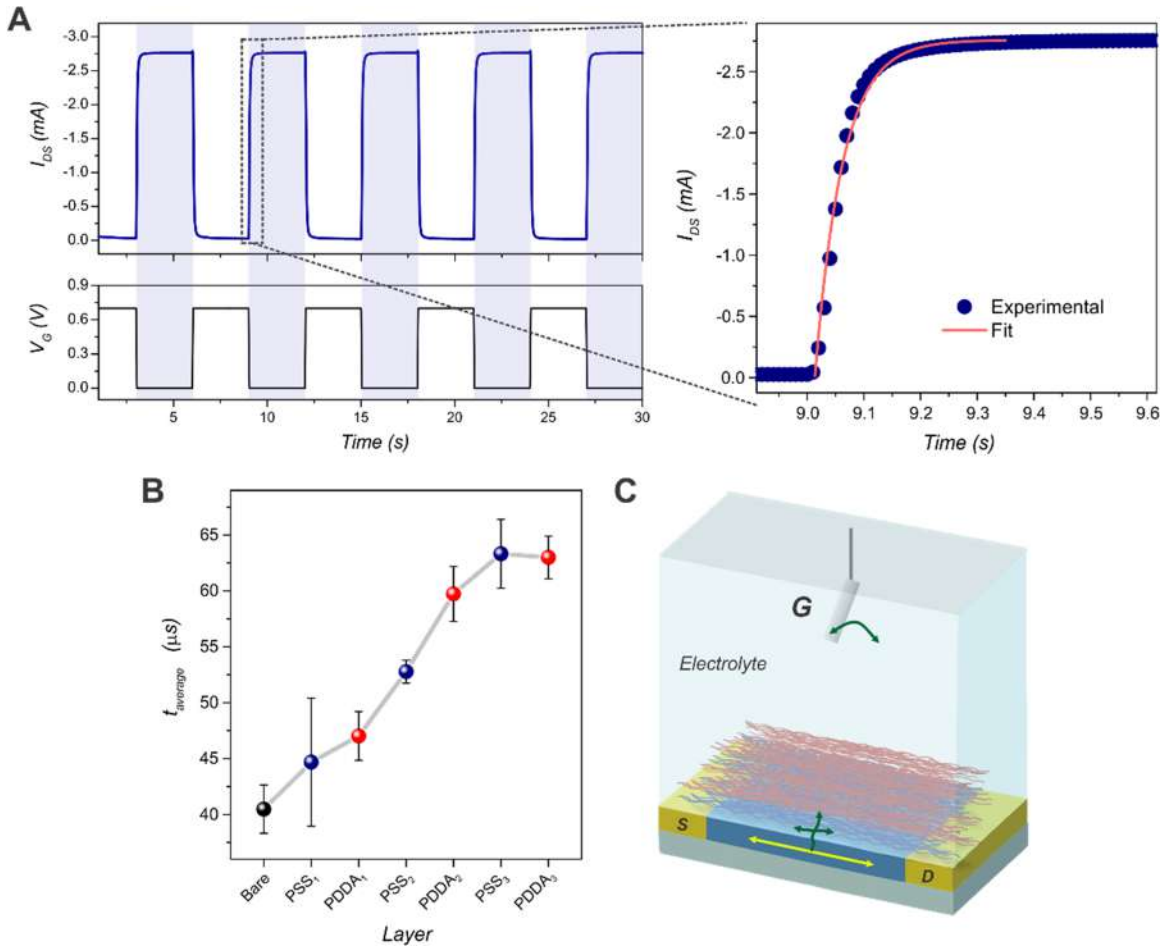

Figure 3. Transient characteristics of a PSS_1-modified OECT (V_D = −0.1 V, KCl 0.1 M) (left) and zoom and fitting to an exponential dependence (right) (A). Average time obtained for PEDOT−PAH OECTs upon subsequent assembling of bilayers. Average of two measurements performed for each switching process (B). Scheme of the different ionic (green arrows) and electronic (yellow arrows) transport occurring during the operation of the OECTs (C).

monitored without a significant alteration of the growth behavior, which is important since it is known that electric fields can affect the deposition of polyelectrolyte multilayers.[29,47] In addition, since the devices present almost optimal transconductance at 0 V gate voltage, they could be further employed for the highly sensitive monitoring of surface processes.

In order to characterize the assembled multilayer films on the OECTs, we followed the LbL assembly process on PEDOT−PAH-modified QCM substrates. From the results in Figure S7 it is inferred that the assembly effectively grows on the PEDOT−PAH-modified substrate, and the thicknesses values of the multilayer assembly are in good accordance with previously reported works.[55] In addition, it is observed that the mass change for the first layer of PSS is markedly higher than the subsequent ones, exhibiting a similar tendency to the one observed in Figure 2(D) and supporting the previously described hypothesis.

It is also relevant to mention that, although the Debye length in the employed electrolyte solution (0.1 M KCl) is 0.96 nm, the fabricated devices displayed responses up to the assembly of the sixth bilayer, which correlates to a film thickness of around 22 nm. A similar phenomenon was reported for polyelectrolytes assembled on graphene-FETs, and it was ascribed to the decrease of effective mobile ions inside the polymer interface onto the semiconducting channel.[56]

Effect of Polyelectrolyte Multilayers on the Transient Behavior. Next, the influence of the multilayer assembly buildup on the transient characteristics of the devices was also studied. With this aim, the reiterated switching of the transistors between the ON and OFF conditions was implemented by the application of a square-wave applied gate potential at a constant drain voltage, while simultaneously recording the drain−source current. As explained elsewhere,[9,57] the t_{on} and t_{off} values were obtained for each modification step by fitting the I_{DS} response of the transistors to an exponential decay. Figure 3(A) and Figure S8 show the transient response for PSS_1-modified and $PDDA_1$-modified PEDOT−PAH OECTs, respectively, together with the exponential fitting curve result for the ON response. Furthermore, t_{on} and t_{off} values are shown in Figure S9, and the average of both values ($t_{average} = (t_{on} + t_{off})/2$) are shown in Figure 3(B).

The average time (as well as the ON and OFF values) increases with the subsequently deposited polymeric layers, and the values reach a plateau for the $PDDA_3$ polyelectrolyte layer. This result accounts for a hindered/worsened ion transport across the film as a result of successive polyelectrolyte incorporation, as previously reported.[9] In this regard, an

https://doi.org/10.1021/acsaelm.2c01124
ACS Appl. Electron. Mater. XXXX, XXX, XXX−XXX

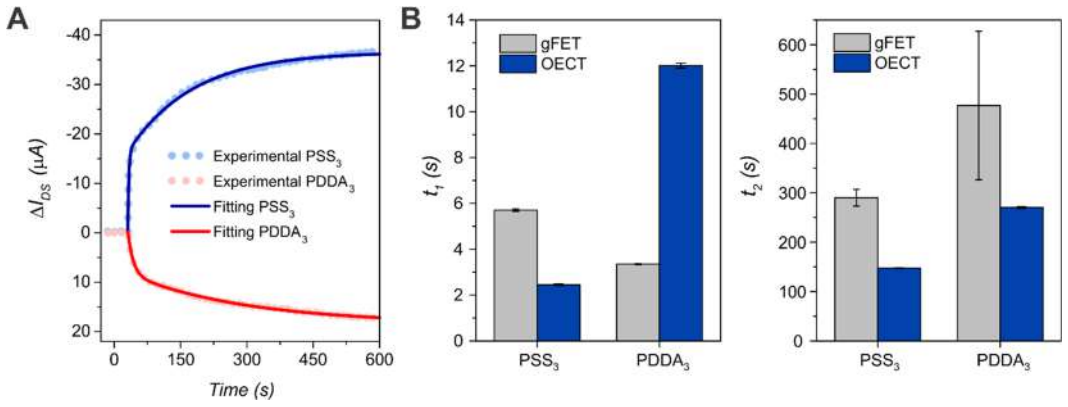

Figure 4. Experimental data and fitting for the monitoring of the third assembled bilayer by OECTs (A). Characteristics times for the third bilayer assembly process obtained from the fitting to the two-step adsorption model and comparison with the same process studied by gFETs (data obtained from ref 53) (B).

electronic circuit comprised of a resistance (electronic transport within the channel) and an ionic circuit along the gate and the channel can be employed in order to describe the behavior of OECTs (Figure 3(C)).[9,57] Therefore, the deposition of each polyelectrolyte layer incorporates a further capacitance to the ionic circuit between the gate electrode and the channel, causing a decrease in the electronic transport efficiency and, consequently, an increase in both t_{on} and t_{off} in the devices, as previously reported.[9,44]

Results observed in Figure S8 show that the nature of the charge of the polyelectrolyte does not affect the shape of the transient behavior of the devices; that is, there is no effect ascribed to the charge exclusion, showing that the process is governed by the exchange of both type of ions. Moreover, it is important to note that, compared to other recently reported OECTs,[58] the obtained $t_{average}$ of 41 μs (for 1:5 dilution OECTs) is remarkably lower. A detailed comparison with previously reported OECTs is presented in Table S1. Interestingly, even when the whole multilayer assembly is deposited on the OECTs, the obtained time (62 μs) continues to be considerably lower than most of those for reported PEDOT-based OECTs, showing that PEDOT−PAH-based OECTs can be modified without significantly affecting their features. Importantly, both obtained times are sufficiently fast for capturing neural activity.[59]

Finally, it can also be noted that the ON and OFF times for the first PSS layer show a similar increase to the ones observed upon the deposition of the subsequent four polyelectrolyte layers, until the plateau is reached for the last one. This average change in the ON and OFF times while assembling the bilayers means that the capacitance (or the blocking effect) added up by each bilayer is almost constant. In contrast, it was shown that the assembly of the polyelectrolyte layers shows different outcomes in I_{DS} values in the real-time measurements, which can be explained by either the change in the conductivity of the channel arising from the doping/dedoping of the PEDOT conducting phase or an electrostatic effect on the surface potential, depending on the assembled layer. These results evidence that the two different electrical measurements yield complementary information from the assembly process taking place on the organic transistors.

Comparison with FET-Based State-of-the-Art Technologies. Since the past decade, graphene field-effect transistors (gFETs) have shown remarkable features for the monitoring of charged macromolecule interactions.[36,37,60] Although OECT technology presents some similarities (i.e., the modulation of a semiconducting channel through the application of a gate voltage through an electrolyte solution), the use of different materials to bridge the source and drain electrodes could lead to differences on the sensing performance. Therefore, the comparison between both devices regarding the monitoring of charged macromolecule adsorption is of great importance toward the developing of biosensing devices.

With this in mind, the results obtained for the real-time monitoring of the LbL assembly of PSS and PDDA by PEDOT−PAH-based OECTs were compared to those previously reported by Scotto et al.[53] by employing gFETs as a sensing platform. For gFETs, it has been demonstrated that the variation of the drain−source current during the adsorption process of a polyelectrolyte layer at a distance d from the surface correlates with the adsorbed mass density, Γ, following the expression $\Delta I_{DS} = A'\Gamma\ e^{-d/\lambda}$, where λ is the Debye length inside the film. Employing this expression, the extended Debye length inside the assembly was estimated, obtaining a value of 9 nm (see the Supporting Information). This value is in very good agreement with the one found for the same assembly on gFETs[53] and explains the capability of the OECT for sensing the polyelectrolyte deposition at distances from the surface 1 order of magnitude greater than the solution Debye length.

Next, through the fitting of the real-time monitoring curves of the LbL assembly, it is possible to study the kinetic features of the polyelectrolyte adsorption with high reliability. The characteristic times associated with the two processes occurring during the polyelectrolyte deposition (one associated with fast adsorption driven by electrostatic interactions between polymer chains with opposite charges and a second one involving an internal reorganization of the film) can be obtained by fitting the FET response to a simple model, considering that $\Gamma_T = \Gamma_1(1 - e^{t/\tau_1}) + \Gamma_2(1 - e^{-t/\tau_2})$,[61] where Γ_1 and Γ_2 correspond to the maximum mass densities adsorbed in each process and τ_1 and τ_2 are the corresponding characteristic times. Moreover, $\Gamma_1 + \Gamma_2 = \Gamma_T$, where Γ_T is the total adsorbed mass density at equilibrium (see the Supporting Information for more details).

Next, following the above-described model, the OECT responses for the third assembled bilayer were fitted to a double-exponential decay (Figure 4(A)). The comparison of the results obtained for the time-resolved responses for the

https://doi.org/10.1021/acsaelm.2c01124
ACS Appl. Electron. Mater. XXXX, XXX, XXX−XXX

adsorption of PDDA and PSS for the two types of FET devices is shown in Figure 4(B) (while the comparison with the gold standard technique SPR is shown in Figure S10). It is observed that both gFET and OECT devices show similar characteristic times for both steps of the polyelectrolyte adsorption process. For both FETs, the first step of the adsorption process (that involves the electrostatic-driven adsorption of the polyelectrolyte) shows τ_1 values lower than 12 s. It is also noted that the second process is faster on OECTs than on gFETs. Therefore, it is evidenced that it is possible to monitor and study the kinetics of the polyelectrolyte adsorption process by employing PEDOT−PAH OECTs in a similar way that it can be done with gFETs, and without the requirement of functionalizing the channel surface with, for instance, pyrene-like molecules.[62]

CONCLUSIONS

We have shown the fabrication of PEDOT−PAH-based OECTs and the monitoring of the LbL assembly process on their surface. To this end, different synthesis conditions were first evaluated in order to optimize the electrical features of the transistors. Next, the OECTs prepared with the 1:5 dilution were chosen, and the polyelectrolyte multilayers assembly process was monitored through the study of the transfer characteristics curves and the change in the drain−source current at constant gate voltage. It was demonstrated that it is possible to detect the assembly of the different layers in real time due to the variations in the effective gate potential upon the deposition of each layer. Subsequently, the study of the transient characteristics upon the assembly of the different layers provided information about the ionic transport through the film during the ON and OFF switching. Taken together, the investigation via the different electrical measurements provided information about the different electronic and ionic transport processes that take place upon the multilayer assembly on the OECTs. Lastly, the real-time response of the OECTs for the assembly of charged macromolecules was fitted to a two-step adsorption model and compared to graphene field-effect transistors and surface plasmon resonance, showing similar results. The monitoring of the alternated assembly of polyelectrolytes results in a straightforward and useful proof-of-concept for the further development of a biosensing FET-based device. By making use of this strategy and through the use of proper bioconjugation techniques, OECT-based sensing devices could be developed toward the real-time detection of analytes ranging from small molecules to a broad variety of biomacromolecules, such as proteins and nucleic acids.

ASSOCIATED CONTENT

Supporting Information

The Supporting Information is available free of charge at https://pubs.acs.org/doi/10.1021/acsaelm.2c01124.

Experimental methods, study of stability of the transistors, QCM measurements, further transient measurements, polyelectrolyte adsorption model, and comparison with other technologies (PDF)

AUTHOR INFORMATION

Corresponding Authors

Gonzalo Eduardo Fenoy − *Instituto de Investigaciones Fisicoquímicas Teóricas y Aplicadas (INIFTA), Departamento de Química, Facultad de Ciencias Exactas, Universidad Nacional de La Plata (UNLP), La Plata 1900, Argentina; AIT Austrian Institute of Technology GmbH, 3430 Tulln an der Donau, Austria*; Email: gonzalofenoy@inifta.unlp.edu.ar

Waldemar Alejandro Marmisollé − *Instituto de Investigaciones Fisicoquímicas Teóricas y Aplicadas (INIFTA), Departamento de Química, Facultad de Ciencias Exactas, Universidad Nacional de La Plata (UNLP), La Plata 1900, Argentina*; Email: wmarmi@inifta.unlp.edu.ar

Authors

Juliana Scotto − *Instituto de Investigaciones Fisicoquímicas Teóricas y Aplicadas (INIFTA), Departamento de Química, Facultad de Ciencias Exactas, Universidad Nacional de La Plata (UNLP), La Plata 1900, Argentina*

Juan A. Allegretto − *Instituto de Investigaciones Fisicoquímicas Teóricas y Aplicadas (INIFTA), Departamento de Química, Facultad de Ciencias Exactas, Universidad Nacional de La Plata (UNLP), La Plata 1900, Argentina*

Esteban Piccinini − *Instituto de Investigaciones Fisicoquímicas Teóricas y Aplicadas (INIFTA), Departamento de Química, Facultad de Ciencias Exactas, Universidad Nacional de La Plata (UNLP), La Plata 1900, Argentina*

Agustín Lorenzo Cantillo − *GISENS BIOTECH, Buenos Aires 1195, Argentina*

Wolfgang Knoll − *AIT Austrian Institute of Technology GmbH, 3430 Tulln an der Donau, Austria; Danube Private University (DPU), Krems 3500, Austria*

Omar Azzaroni − *Instituto de Investigaciones Fisicoquímicas Teóricas y Aplicadas (INIFTA), Departamento de Química, Facultad de Ciencias Exactas, Universidad Nacional de La Plata (UNLP), La Plata 1900, Argentina*

Complete contact information is available at: https://pubs.acs.org/10.1021/acsaelm.2c01124

Author Contributions

The manuscript was written through contributions of all authors. All authors have given approval to the final version of the manuscript. G.E.F. and J.S. contributed equally.

Funding

This work was supported by the following institutions: Universidad Nacional de La Plata (PID-X867), ANPCYT (PICT 2018-04684), GISENS BIOTECH, and CONICET-UNLP-GISENS BIOTECH (700-2845/20-000).

Notes

The authors declare the following competing financial interest(s): E.P., W.A.M., and O.A. are scientific advisors of GISENS BIOTECH through a contract between UNLP, CONICET, and GISENS BIOTECH. A.L.C. is recently or presently employed by GISENS BIOTECH. The other authors declare no competing interests.

ACKNOWLEDGMENTS

G.E.F. acknowledges OeAD for an Ernst Mach Grant scholarship. G.E.F. and J.A.A. acknowledge CONICET for a scholarship. J.S., E.P., W.A.M., and O.A. are staff members of CONICET.

REFERENCES

(1) Simon, D. T.; Gabrielsson, E. O.; Tybrandt, K.; Berggren, M. Organic Bioelectronics: Bridging the Signaling Gap between Biology and Technology. *Chem. Rev.* **2016**, *116* (21), 13009−13041.

(2) Pitsalidis, C.; Pappa, A. M.; Boys, A. J.; Fu, Y.; Moysidou, C. M.; Van Niekerk, D.; Saez, J.; Savva, A.; Iandolo, D.; Owens, R. M. Organic Bioelectronics for in Vitro Systems. *Chem. Rev.* **2022**, *122* (4), 4700−4790.

(3) Rivnay, J.; Owens, R. M.; Malliaras, G. G. The Rise of Organic Bioelectronics. *Chem. Mater.* **2014**, *26* (1), 679−685.

(4) Fenoy, G. E.; Azzaroni, O.; Knoll, W.; Marmisollé, W. A. Functionalization Strategies of PEDOT and PEDOT:PSS Films for Organic Bioelectronics Applications. *Chemosensors* **2021**, *9* (8), 212.

(5) Berggren, M.; Głowacki, E. D.; Simon, D. T.; Stavrinidou, E.; Tybrandt, K. In Vivo Organic Bioelectronics for Neuromodulation. *Chem. Rev.* **2022**, *122* (4), 4826−4846.

(6) Marks, A.; Griggs, S.; Gasparini, N.; Moser, M. Organic Electrochemical Transistors: An Emerging Technology for Biosensing. *Adv. Mater. Interfaces* **2022**, *9* (6), 2102039.

(7) Smela, E. Conjugated Polymer Actuators for Biomedical Applications. *Adv. Mater.* **2003**, *15* (6), 481−494.

(8) Bianchi, M.; De Salvo, A.; Asplund, M.; Carli, S.; Di Lauro, M.; Schulze-Bonhage, A.; Stieglitz, T.; Fadiga, L.; Biscarini, F. Poly(3,4-ethylenedioxythiophene)-Based Neural Interfaces for Recording and Stimulation: Fundamental Aspects and In Vivo Applications. *Adv. Sci.* **2022**, *2104701*, 2104701.

(9) Fenoy, G. E.; Bilderling, C.; Knoll, W.; Azzaroni, O.; Marmisollé, W. A. PEDOT:Tosylate-Polyamine-Based Organic Electrochemical Transistors for High-Performance Bioelectronics. *Adv. Electron. Mater.* **2021**, *7* (6), 2100059.

(10) Strakosas, X.; Bongo, M.; Owens, R. M. The Organic Electrochemical Transistor for Biological Applications. *J. Appl. Polym. Sci.* **2015**, *132* (15), 1−14.

(11) Berggren, M.; Richter-Dahlfors, A. Organic Bioelectronics. *Adv. Mater.* **2007**, *19* (20), 3201−3213.

(12) Rivnay, J.; Inal, S.; Salleo, A.; Owens, R. M.; Berggren, M.; Malliaras, G. G. Organic Electrochemical Transistors. *Nat. Rev. Mater.* **2018**, *3*, 17086.

(13) Ting, S.; Tan, M.; Keene, S.; Giovannitti, A.; Melianas, A.; Moser, M.; Salleo, A. *Operation Mechanism of Organic Electrochemical Transistors as Redox Chemical Transducers †*. **2021**, *9*, 12148−12158.

(14) Khodagholy, D.; Rivnay, J.; Sessolo, M.; Gurfinkel, M.; Leleux, P.; Jimison, L. H.; Stavrinidou, E.; Herve, T.; Sanaur, S.; Owens, R. M.; Malliaras, G. G. High Transconductance Organic Electrochemical Transistors. *Nat. Commun.* **2013**, *4*, 1−6.

(15) Berggren, M.; Crispin, X.; Fabiano, S.; Jonsson, M. P.; Simon, D. T.; Stavrinidou, E.; Tybrandt, K.; Zozoulenko, I. Ion Electron-Coupled Functionality in Materials and Devices Based on Conjugated Polymers. *Adv. Mater.* **2019**, *1805813*, 1−15.

(16) Zeglio, E.; Inganäs, O. Active Materials for Organic Electrochemical Transistors. *Adv. Mater.* **2018**, *30* (44), 1−18.

(17) Inal, S.; Malliaras, G. G.; Rivnay, J. Benchmarking Organic Mixed Conductors for Transistors. *Nat. Commun.* **2017**, *8* (1), 1−6.

(18) Keene, S. T.; van der Pol, T. P. A.; Zakhidov, D.; Weijtens, C. H. L.; Janssen, R. A. J.; Salleo, A.; van de Burgt, Y. Enhancement-Mode PEDOT:PSS Organic Electrochemical Transistors Using Molecular De-Doping. *Adv. Mater.* **2020**, *32* (19), 2000270.

(19) Minudri, D.; Mantione, D.; Dominguez-Alfaro, A.; Moya, S.; Maza, E.; Bellacanzone, C.; Antognazza, M. R.; Mecerreyes, D. Water Soluble Cationic Poly(3,4-Ethylenedioxythiophene) PEDOT-N as a Versatile Conducting Polymer for Bioelectronics. *Adv. Electron. Mater.* **2020**, *6* (10), 1−10.

(20) Mantione, D.; del Agua, I.; Sanchez-Sanchez, A.; Mecerreyes, D. Poly(3,4-Ethylenedioxythiophene) (PEDOT) Derivatives: Innovative Conductive Polymers for Bioelectronics. *Polymers (Basel).* **2017**, *9* (8), 354.

(21) Donahue, M. J.; Sanchez-Sanchez, A.; Inal, S.; Qu, J.; Owens, R. M.; Mecerreyes, D.; Malliaras, G. G.; Martin, D. C. Tailoring PEDOT Properties for Applications in Bioelectronics. *Mater. Sci. Eng. R Reports* **2020**, *140*, 100546.

(22) Huang, L.; Yang, X.; Deng, L.; Ying, D.; Lu, A.; Zhang, L.; Yu, A.; Duan, B. Biocompatible Chitin Hydrogel Incorporated with PEDOT Nanoparticles for Peripheral Nerve Repair. *ACS Appl. Mater. Interfaces* **2021**, *13* (14), 16106−16117.

(23) Fabiano, S.; Braun, S.; Liu, X.; Weverberghs, E.; Gerbaux, P.; Fahlman, M.; Berggren, M.; Crispin, X. Poly(Ethylene Imine) Impurities Induce n-Doping Reaction in Organic (Semi)Conductors. *Adv. Mater.* **2014**, *26* (34), 6000−6006.

(24) Cea, C.; Spyropoulos, G. D.; Jastrzebska-Perfect, P.; Ferrero, J. J.; Gelinas, J. N.; Khodagholy, D. Enhancement-Mode Ion-Based Transistor as a Comprehensive Interface and Real-Time Processing Unit for in Vivo Electrophysiology. *Nat. Mater.* **2020**, *19* (6), 679−686.

(25) Decher, G. Fuzzy Nanoassemblies: Toward Layered Polymeric Multicomposites. *Science (80-.).* **1997**, *277* (5330), 1232−1237.

(26) Decher, G.; Hong, J. D.; Schmitt, J. Buildup of Ultrathin Multilayer Films by a Self-Assembly Process: III. Consecutively Alternating Adsorption of Anionic and Cationic Polyelectrolytes on Charged Surfaces. *Thin Solid Films* **1992**, *210−211*, 831−835.

(27) Fenoy, G. E.; Van der Schueren, B.; Scotto, J.; Boulmedais, F.; Ceolín, M. R.; Bégin-Colin, S.; Bégin, D.; Marmisollé, W. a.; Azzaroni, O. Layer-by-Layer Assembly of Iron Oxide-Decorated Few-Layer Graphene/PANI:PSS Composite Films for High Performance Supercapacitors Operating in Neutral Aqueous Electrolytes. *Electrochim. Acta* **2018**, *283*, 1178−1187.

(28) Fenoy, G. E.; Rafti, M.; Marmisollé, W. A.; Azzaroni, O. Nanoarchitectonics of Metal Organic Frameworks and PEDOT Layer-by-Layer Electrodes for Boosting Oxygen Reduction Reaction. *Mater. Adv.* **2021**, *2*, 7731−7740.

(29) Richardson, J. J.; Cui, J.; Björnmalm, M.; Braunger, J. A.; Ejima, H.; Caruso, F. Innovation in Layer-by-Layer Assembly. *Chem. Rev.* **2016**, *116* (23), 14828−14867.

(30) Luo, J.; Liu, R.; Liu, X. Layer-by-Layer Assembled Ionic-Liquid Functionalized Graphene/Polyaniline Nanocomposite with Enhanced Electrochemical Sensing Properties. *J. Mater. Chem. C* **2014**, *2*, 4818−4827.

(31) Ariga, K.; Yamauchi, Y. Nanoarchitectonics from Atom to Life. *Chem. - An Asian J.* **2020**, *15* (6), 718−728.

(32) Fenoy, G. E.; Maza, E.; Zelaya, E.; Marmisollé, W. A.; Azzaroni, O. Layer-by-Layer Assemblies of Highly Connected Polyelectrolyte Capped-Pt Nanoparticles for Electrocatalysis of Hydrogen Evolution Reaction. *Appl. Surf. Sci.* **2017**, *416* (1650), 24−32.

(33) Vander Straeten, A.; Bratek-Skicki, A.; Jonas, A. M.; Fustin, C. A.; Dupont-Gillain, C. C. Integrating Proteins in Layer-by-Layer Assemblies Independently of Their Electrical Charge. *ACS Nano* **2018**, *12* (8), 8372−8381.

(34) Ariga, K.; Yamauchi, Y.; Rydzek, G.; Ji, Q.; Yonamine, Y.; Wu, K. C.-W.; Hill, J. P. Layer-by-Layer Nanoarchitectonics: Invention, Innovation, and Evolution. *Chem. Lett.* **2014**, *43* (1), 36−68.

(35) Guzmán, E.; Rubio, R. G.; Ortega, F. A Closer Physico-Chemical Look to the Layer-by-Layer Electrostatic Self-Assembly of Polyelectrolyte Multilayers. *Adv. Colloid Interface Sci.* **2020**, *282*, 102197.

(36) Aspermair, P.; Ramach, U.; Reiner-Rozman, C.; Fossati, S.; Lechner, B.; Moya, S. E.; Azzaroni, O.; Dostalek, J.; Szunerits, S.; Knoll, W.; Bintinger, J. Dual Monitoring of Surface Reactions in Real Time by Combined Surface-Plasmon Resonance and Field-Effect Transistor Interrogation. *J. Am. Chem. Soc.* **2020**, *142* (27), 11709−11716.

(37) Piccinini, E.; Alberti, S.; Longo, G. S.; Berninger, T.; Breu, J.; Dostalek, J.; Azzaroni, O.; Knoll, W. Pushing the Boundaries of Interfacial Sensitivity in Graphene FET Sensors: Polyelectrolyte Multilayers Strongly Increase the Debye Screening Length. *J. Phys. Chem. C* **2018**, *122* (18), 10181−10188.

(38) Fenoy, G. E.; Marmisollé, W. A.; Azzaroni, O.; Knoll, W. Acetylcholine Biosensor Based on the Electrochemical Functionaliza-

https://doi.org/10.1021/acsaelm.2c01124
ACS Appl. Electron. Mater. XXXX, XXX, XXX−XXX

tion of Graphene Field-Effect Transistors. *Biosens. Bioelectron.* **2020**, *148*, 111796.
(39) Fu, W.; Jiang, L.; van Geest, E. P.; Lima, L. M. C.; Schneider, G. F. Sensing at the Surface of Graphene Field-Effect Transistors. *Adv. Mater.* **2017**, *29* (6), 1603610.
(40) Bernards, D. A.; Macaya, D. J.; Nikolou, M.; Defranco, J. A.; Takamatsu, S.; Malliaras, G. G. *Enzymatic Sensing with Organic Electrochemical Transistors.* **2008**, *18*, 116−120.
(41) Macchia, E.; Romele, P.; Manoli, K.; Ghittorelli, M.; Magliulo, M. Ultra-Sensitive Protein Detection with Organic Electrochemical Transistors Printed on Plastic Substrate. *Flex. Print. Electron.* **2018**, *3*, 034002.
(42) Koklu, A.; Wustoni, S.; Musteata, V. E.; Ohayon, D.; Moser, M.; McCulloch, I.; Nunes, S. P.; Inal, S. Microfluidic Integrated Organic Electrochemical Transistor with a Nanoporous Membrane for Amyloid-β Detection. *ACS Nano* **2021**, *15* (5), 8130−8141.
(43) Hai, W.; Goda, T.; Takeuchi, H.; Yamaoka, S.; Horiguchi, Y.; Matsumoto, A.; Miyahara, Y. Human Influenza Virus Detection Using Sialyllactose-Functionalized Organic Electrochemical Transistors. *Sensors Actuators, B Chem.* **2018**, *260*, 635−641.
(44) Pappa, A. M.; Inal, S.; Roy, K.; Zhang, Y.; Pitsalidis, C.; Hama, A.; Pas, J.; Malliaras, G. G.; Owens, R. M. Polyelectrolyte Layer-by-Layer Assembly on Organic Electrochemical Transistors. *ACS Appl. Mater. Interfaces* **2017**, *9* (12), 10427−10434.
(45) Rivnay, J.; Leleux, P.; Sessolo, M.; Khodagholy, D.; Hervé, T.; Fiocchi, M.; Malliaras, G. G. Organic Electrochemical Transistors with Maximum Transconductance at Zero Gate Bias. *Adv. Mater.* **2013**, *25* (48), 7010−7014.
(46) Yu, S.; Ratcliff, E. L. Tuning Organic Electrochemical Transistor (OECT) Transconductance toward Zero Gate Voltage in the Faradaic Mode. *ACS Appl. Mater. Interfaces* **2021**, *13* (42), 50176−50186.
(47) Ko, Y. H.; Kim, Y. H.; Park, J.; Nam, K. T.; Park, J. H.; Yoo, P. J. Electric-Field-Assisted Layer-by-Layer Assembly of Weakly Charged Polyelectrolyte Multilayers. *Macromolecules* **2011**, *44* (8), 2866−2872.
(48) Zhou, Y.; Fuentes-Hernandez, C.; Shim, J.; Meyer, J.; Giordano, A. J.; Li, H.; Winget, P.; Papadopoulos, T.; Cheun, H.; Kim, J.; Fenoll, M.; Dindar, A.; Haske, W.; Najafabadi, E.; Khan, T. M.; Sojoudi, H.; Barlow, S.; Graham, S.; Brédas, J. L.; Marder, S. R.; Kahn, A.; Kippelen, B. A Universal Method to Produce Low-Work Function Electrodes for Organic Electronics. *Science (80-.).* **2012**, *336* (6079), 327−332.
(49) Liu, A.; Anzai, J. I. Ferrocene-Containing Polyelectrolyte Multilayer Films: Effects of Electrochemically Inactive Surface Layers on the Redox Properties. *Langmuir* **2003**, *19* (9), 4043−4046.
(50) Calvo, E. J.; Wolosiuk, A. Donnan Permselectivity in Layer-by-Layer Self-Assembled Redox Polyelectrolye Thin Films. *J. Am. Chem. Soc.* **2002**, *124* (28), 8490−8497.
(51) Sukhorukov, G. B.; Donath, E.; Lichtenfeld, H.; Knippel, E.; Knippel, M.; Budde, A.; Möhwald, H. Layer-by-Layer Self Assembly of Polyelectrolytes on Colloidal Particles. *Colloids Surfaces A Physicochem. Eng. Asp.* **1998**, *137* (1), 253−266.
(52) Borges, J.; Mano, J. F. Molecular Interactions Driving the Layer-by-Layer Assembly of Multilayers. *Chem. Rev.* **2014**, *114* (18), 8883−8942.
(53) Scotto, J.; Cantillo, A. L.; Piccinini, E.; Fenoy, G. E.; Allegretto, J. A.; Piccinini, J. M.; Marmisollé, W. A.; Azzaroni, O. Using Graphene Field-Effect Transistors for Real-Time Monitoring of Dynamic Processes at Sensing Interfaces. Benchmarking Performance against Surface Plasmon Resonance. *ACS Appl. Electron. Mater.* **2022**, *4* (8), 3988−3996.
(54) Poghossian, A.; Abouzar, M. H.; Sakkari, M.; Kassab, T.; Han, Y.; Ingebrandt, S.; Offenhäusser, A.; Schöning, M. J. Field-Effect Sensors for Monitoring the Layer-by-Layer Adsorption of Charged Macromolecules. *Sensors Actuators, B Chem.* **2006**, *118* (1−2), 163−170.
(55) Iturri Ramos, J. J.; Stahl, S.; Richter, R. P.; Moya, S. E. Water Content and Buildup of Poly(Diallyldimethylammonium Chloride)/Poly(Sodium 4-Styrenesulfonate) and Poly(Allylamine Hydrochloride)/Poly(Sodium 4-Styrenesulfonate) Polyelectrolyte Multilayers Studied by an in Situ Combination of a Quartz Crystal Microb. *Macromolecules* **2010**, *43* (21), 9063−9070.
(56) Piccinini, E.; Alberti, S.; Longo, G. S.; Berninger, T.; Breu, J.; Dostalek, J.; Azzaroni, O.; Knoll, W. Pushing the Boundaries of Interfacial Sensitivity in Graphene FET Sensors: Polyelectrolyte Multilayers Strongly Increase the Debye Screening Length. *J. Phys. Chem. C* **2018**, *122* (18), 10181−10188.
(57) Faria, G. C.; Duong, D. T.; Salleo, A. On the Transient Response of Organic Electrochemical Transistors. *Org. Electron.* **2017**, *45*, 215−221.
(58) Paudel, P. R.; Skowrons, M.; Dahal, D.; Radha Krishnan, R. K.; Lüssem, B. The Transient Response of Organic Electrochemical Transistors. *Adv. Theory Simulations* **2022**, *2100563*, 1−15.
(59) Khodagholy, D.; Gurfinkel, M.; Stavrinidou, E.; Leleux, P.; Herve, T.; Sanaur, S.; Malliaras, G. G. High Speed and High Density Organic Electrochemical Transistor Arrays. *Appl. Phys. Lett.* **2011**, *99* (16), 163304.
(60) Piccinini, E.; Fenoy, G. E.; Cantillo, A. L.; Allegretto, J. A.; Scotto, J.; Piccinini, J. M.; Marmisollé, W. A.; Azzaroni, O. Biofunctionalization of Graphene-Based FET Sensors through Heterobifunctional Nanoscaffolds: Technology Validation toward Rapid COVID-19 Diagnostics and Monitoring. *Adv. Mater. Interfaces* **2022**, *9* (15), 2102526.
(61) Guzmán, E.; Ritacco, H.; Ortega, F.; Svitova, T.; Radke, C. J.; Rubio, R. G. Adsorption Kinetics and Mechanical Properties of Ultrathin Polyelectrolyte Multilayers: Liquid-Supported versus Solid-Supported Films. *J. Phys. Chem. B* **2009**, *113* (20), 7128−7137.
(62) Bottari, G.; Herranz, M. Á.; Wibmer, L.; Volland, M.; Rodríguez-Pérez, L.; Guldi, D. M.; Hirsch, A.; Martín, N.; D'Souza, F.; Torres, T. Chemical Functionalization and Characterization of Graphene-Based Materials. *Chem. Soc. Rev.* **2017**, *46*, 4464−4500.

https://doi.org/10.1021/acsaelm.2c01124
ACS Appl. Electron. Mater. XXXX, XXX, XXX−XXX